



OPEN

# Chloroplast development at low temperature requires the pseudouridine synthase gene *TCD3* in rice

Dongzhi Lin<sup>1</sup>, Rongrong Kong<sup>1</sup>, Lu Chen<sup>1</sup>, Yulu Wang<sup>1</sup>, Lanlan Wu<sup>1</sup>, Jianlong Xu<sup>2</sup>, Zhongze Piao<sup>3</sup>, Gangseob Lee<sup>4</sup> & Yanjun Dong<sup>1,5</sup>✉

Low temperature affects a broad spectrum of cellular components in plants, such as chloroplasts, as well as plant metabolism. On the other hand, pseudouridine ( $\Psi$ ) synthases are required for the most abundant post-transcriptional modification of RNA in *Escherichia coli*. However, the role of rice  $\Psi$  synthases in regulating chloroplast development at low temperature remains elusive. In this study, we identified the rice thermo-sensitive chlorophyll-deficient (*tcd3*) mutant, which displays an albino phenotype before the 4-leaf stage and ultimately dies when grown at 20 °C, but can grow normally at 32 °C. Genetic analysis showed that the mutant trait is controlled by a single recessive nuclear gene (*tcd3*). Map-based cloning, complementation and knockout tests revealed that *TCD3* encodes a chloroplast-localized  $\Psi$  synthase. *TCD3* is a cold-induced gene that is mainly expressed in leaves. The disruption of *TCD3* severely affected the transcript levels of various chloroplast-associated genes, as well as ribosomal genes involved in chloroplast rRNA assembly at low temperature (20 °C), whereas the transcript levels of these genes were normal at high temperature (32 °C). These results provide a first glimpse into the importance of rice  $\Psi$  synthase gene in chloroplast development at low temperatures.

Rice is one of the most important food crops worldwide. Its yield potential is limited by the photosynthetic capacity of leaves that, as carbohydrate factories, are unable to fill the larger number of florets of modern rice plants<sup>1</sup>. The development of intact chloroplasts, a prerequisite for photosynthesis, is affected by environmental factors such as temperature and light. Chloroplast development, a complex process that is coordinately regulated by plastid and nuclear genes, can be divided into three stages<sup>2–4</sup>: (i) the activation of plastid replication and plastid DNA synthesis; (ii) chloroplast “build-up”, characterized by the establishment of the chloroplast genetic system; and (iii) the expression of plastid and nuclear genes for the photosynthetic apparatus. In higher plants, chloroplast genes are transcribed by two types of RNA polymerase: nucleus-encoded polymerases (NEP) and plastid-encoded polymerases (PEP). NEPs are mainly responsible for transcribing the components of the transcriptional/translational machinery, such as *rpoA* and *rpoB*, while PEPs are required for the transcription of photosynthetic genes such as *psbA*, *psbD*, and *rbcL*. Mutations of those genes directly or indirectly affect chlorophyll biosynthesis or degradation pathways as well as photosynthesis, ultimately resulting in differences in leaf color or even plant death<sup>5–9</sup>. However, the roles of the many genes in the regulation of chloroplast development in higher plants remain largely unknown<sup>10</sup>.

Pseudouridine (5-ribosyluracil;  $\Psi$ ) synthases, responsible for the most abundant post-transcriptional modification of cellular RNAs (pseudouridine), share a common core fold and active site structure. This core structure is modified by peripheral domains comprising accessory proteins with different amino acid sequences (depending on the family) and guide RNAs, giving rise to remarkable substrate versatility. These synthases catalyze the site-specific isomerization of uridine residues in the RNA chain and appear to employ both sequence and structural information to achieve site specificity<sup>11</sup>. All  $\Psi$  synthases identified to date from Archaea, Bacteria, and

<sup>1</sup>College of Life Sciences, Shanghai Normal University, Shanghai, 200234, China. <sup>2</sup>The Institute of Crop Sciences, Chinese Academy of Agricultural Sciences, 12 South Zhong-Guan Cun Street, Beijing, 100081, China. <sup>3</sup>Crop Breeding and Cultivation Research Institute, Shanghai Academy of Agricultural Sciences, 1000 Jingqi Road, Fengxian District, Shanghai, 201403, China. <sup>4</sup>National Institute of Agricultural Science, Jeon Ju, 560-500, Korea. <sup>5</sup>Shanghai Key Laboratory of Plant Molecular Sciences, Shanghai, 200234, China. ✉e-mail: [dong@shnu.edu.cn](mailto:dong@shnu.edu.cn)

Eukarya can be classified into five families (RluA, RsuA, TruA, TruB, and TruD)<sup>12</sup>. The most well studied are from *Escherichia coli*, which contains 11  $\Psi$  synthases. Of these, RsuA, RluE, RluB, and RluF belong to the RsuA family; RluA, RluC, RluD, and TruC belong to the RluA family; and TruA, TruB, and TruD are the sole members of their respective families. All of these synthases are site specific, and no overlapping functions have been detected<sup>12,13</sup>. For instance, RsuA isomerizes U516 in ribosomal RNA (rRNA), which is responsible for the universally conserved  $\Psi$ 55 in the T $\Psi$ C loops of all elongator tRNAs in a cell. RluA modifies two structurally distinct types of RNA at positions that share local sequence and structural similarity. TruA and RluD modify several nearby sites on a specific RNA<sup>11</sup>. Nevertheless, the modes of action of  $\Psi$  synthases remain largely unclear, especially during plant growth and development. *Chlamydomonas reinhardtii* *Maa2*, encoding a  $\Psi$  synthase, is involved in chloroplast group II intron trans-splicing of *psaA* RNA; its mutant (*maa2*) cannot grow phototrophically and is highly photosensitive<sup>14</sup>. The *Arabidopsis thaliana*  $\Psi$  synthase SVR1 (At2g39140) is required for normal chloroplast translation<sup>15</sup>. However, to our knowledge, no rice mutants for  $\Psi$  synthase genes have been reported, and the roles of these genes in rice are unknown.

Here, we identified *tcd3*, a mutant of a pseudouridine ( $\Psi$ ) synthase gene in rice that displays thermo-sensitive changes in leaf color under cold stress. The chloroplast-localized  $\Psi$  synthase TCD3 appears to play an essential role in chloroplast development at low temperature in rice.

## Results

**Phenotypic characterization of the *tcd3* mutant.** We observed the leaf color of wild-type (WT) and *tcd3* seedlings grown at two different temperatures, 20 °C and 32 °C (Fig. 1A,B). The *tcd3* seedlings displayed yellowish white leaves and died after the 5-leaf stage when grown at 20 °C. However, when grown at 32 °C, the seedlings remained green, as did WT seedlings at both temperatures. These results indicate that the variation in leaf color of the *tcd3* mutant is controlled by temperature and that this mutant has low-temperature-sensitive characteristics. Consistent with this conclusion, the photosynthetic pigments chlorophyll (Chl) a and b and carotenoid (Car) were almost undetectable in *tcd3* seedlings grown at 20 °C (Fig. 2A), whereas there was only a slight difference in pigment levels between WT and *tcd3* at 32 °C (Fig. 2B). These results indicate that *tcd3* exhibits low levels of photosynthetic pigment biosynthesis at 20 °C, but can quickly recover to almost WT levels at 32 °C. As expected, the structure of WT chloroplasts was complete in seedlings grown at both 32 °C and 20 °C. However, at 20 °C, almost no intact chloroplasts and numerous bubble-like structures were observed in *tcd3* (Fig. 1D), whereas *tcd3* at 32 °C and WT chloroplasts appeared similar (Fig. 1C,E,F). These results indicate that the *tcd3* mutation blocks chloroplast development under cold stress. Interestingly, under field conditions, the leaf Chl contents in *tcd3* plants were indistinguishable from those of WT plants (Fig. S1). In addition, except for a significant reduction in panicle number and grain number, no obvious differences in other traits were observed between *tcd3* and WT plants (Fig. S2), implying that the *tcd3* mutation has a somewhat negative affect on the later stages of plant growth.

**Map-based cloning of TCD3.** Genetic analysis showed that the *tcd3* mutant trait was caused by a recessive mutation based on the approximately 3 (green): 1 (yellowish white) ratio for phenotypic segregation in an F<sub>2</sub> population generated from Peiai64S/*tcd3* (Table S1). As a first step, we selected 236 mutant individuals in the F<sub>2</sub> population and mapped TCD3 between markers MM0541 and RM14407 on chromosome 3 (Fig. 3A). To further fine-map TCD3, we examined 5020 F<sub>2</sub> mutant individuals and developed five InDel molecular markers (Table S2). Ultimately, TCD3 was localized to a 179-kb region between markers ID2738 and ID2917 (Fig. 3B) spanning two BACs (AC105734, AC137635). Based on the Rice Genome Annotation Project (<http://www.rice.plantbiology.msu.edu/>), 32 candidate genes are predicted to be present in the target region, including one encoding a pseudouridine ( $\Psi$ ) synthase (*LOC\_Os3g05806*). We sequenced and analyzed all candidate genes and found only a G-to-A mutation at the 50<sup>th</sup> base pair (bp) and a 5-bp deletion mutation (TCTTG) at bp 51 to 55 in the fifth exon of *LOC\_Os3g05806* (Fig. 3C), which led to a premature translational stop and a frame-shift mutation, respectively.

**Complementation and knockout of TCD3.** To verify that the yellowish white phenotype of *tcd3* at 20 °C is due to the mutation of *LOC\_Os3g05806*, we performed genetic complementation of the *tcd3* mutant and CRISPR/Cas9 genome editing of WT plants. In the complementation test, to quickly obtain results, we induced the differentiation of rice callus at 20 °C. The resulting T<sub>0</sub> transgenic seedlings harboring pCAMBIA1301:TCD3 appeared green (Fig. 1H), whereas non-transgenic seedlings remained yellow (Fig. 1G), indicating that *LOC\_Os3g05806* can rescue the mutant phenotype. In addition, we obtained 19 independent transgenic (T<sub>0</sub>) plants transformed with pCAMBIA1301:TCD3. At 20 °C, we detected segregation of the mutant phenotype in the transgenic plant population (T<sub>1</sub>) and found that all green seedlings contained the transgene (Fig. 1I). As controls, we produced 14 independent lines transformed with the empty vector pCAMBIA1301, which failed to rescue the *tcd3* mutant phenotype. Via CRISPR/Cas9, we obtained 13 transgenic T<sub>0</sub> plants carrying one editing mutation of the 1-bp (G) deletion at 89 bp from the ATG start codon in TCD3 (Fig. S3). Importantly, all homozygous genome-edited T<sub>1</sub> lines exhibited the same mutant phenotype as *tcd3* mutant at 20 °C (Fig. 1J). Taken together, these results confirm that *LOC\_Os3g05806* is TCD3.

**Expression analysis and subcellular localization of TCD3.** We examined the mRNA levels of TCD3 by quantitative RT-PCR in various organs, including seedlings, roots, stems, leaves, and panicles, finding that TCD3 was mainly expressed in leaves. Lower expression levels were also detected in roots, stems, and panicles (Fig. 4A). These results support the notion that TCD3 plays an important role in leaf development, which is consistent with the rice gene expression profiling data (<http://ricexpro.dna.affrc.go.jp/>). To further investigate the effects of temperature on TCD3 expression, we measured TCD3 transcript levels in *tcd3* and WT seedlings at the 3-leaf stage grow, indicating that TCD3 is a cold-inducible gene.

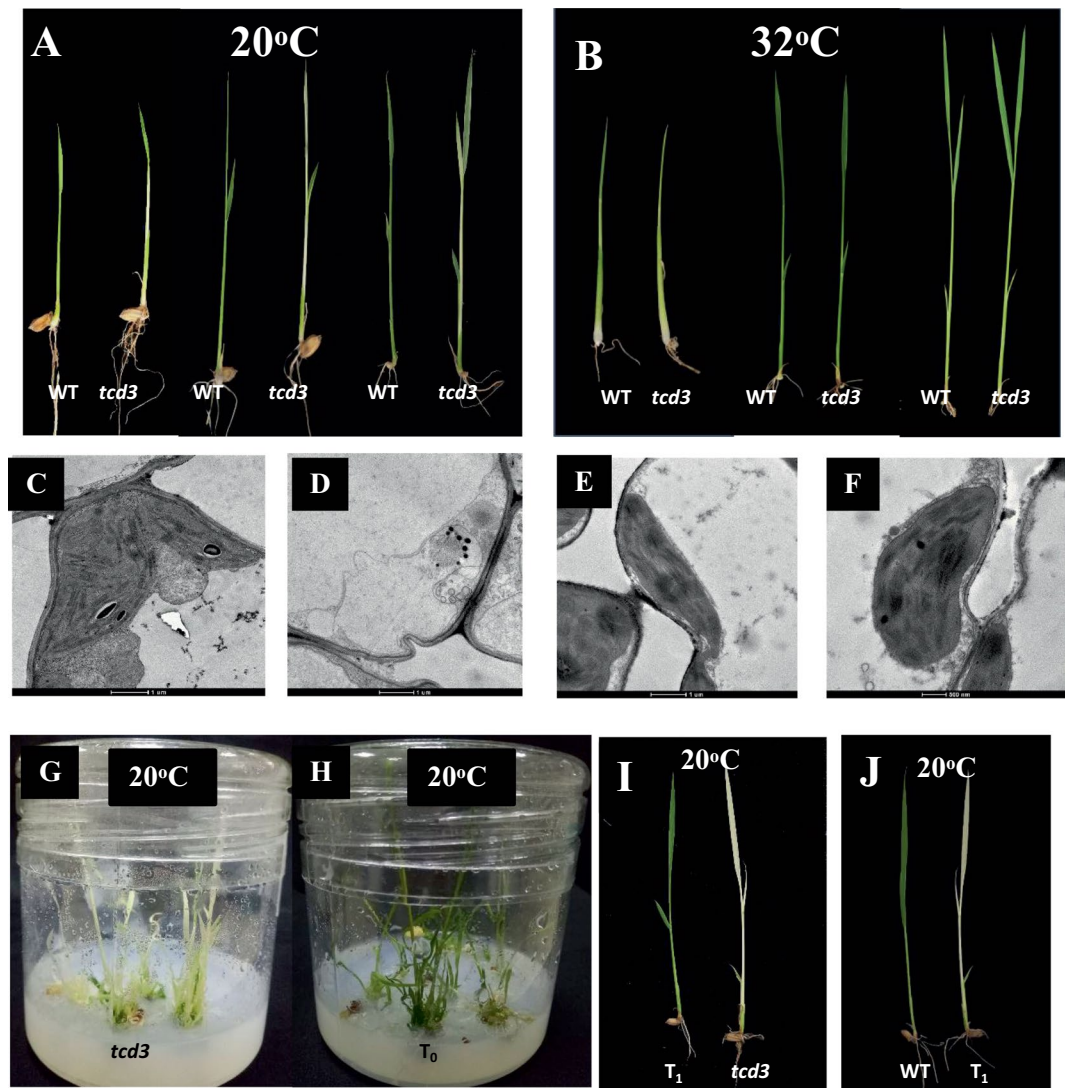


**Figure 1.** Characters of the *tcd3* mutant and WT plants; seedling leaf color in WT and *tcd3* at 20° (A) and 32° (B); chloroplast structure in WT at 20° (C) and 32° (E) and chloroplast structure in *tcd3* at 20° (D) and 32° (F); T<sub>0</sub> complemented plants in the *tcd3* mutant (G) and control (H) backgrounds at 20° of the temperature of differentiation; segregation of T<sub>1</sub> plants obtained from transgenic T<sub>0</sub> plants transformed with pCAMBIA1301-TCD3 (I) and by CRISPR/Cas9 genome editing (J).

The *TCD3* protein was predicted to be localized to the chloroplast according to TargetP (<http://www.cbs.dtu.dk/services/TargetP/>)<sup>16</sup>. To determine the actual subcellular localization of TCD3, we transiently expressed a constitutively transcribed TCD3:GFP fusion construct (35 S:TCD3:GFP) in tobacco cells. The GFP signals from TCD3:GFP were localized to chloroplasts (Fig. 5B). These findings confirm that TCD3 is localized to the chloroplast and is induced under cold stress.

**Characterization of TCD3 protein by bioinformatic analysis.** *TCD3* consists of eight exons and nine introns (Fig. 3C) and encodes a 415 amino-acid protein with a molecular mass of approximately 45 kDa. A search of the Pfam database<sup>17</sup> revealed that TCD3 not only contains a chloroplast transit peptide (CTP; 70 aa), but it also contains an S4 domain and a  $\Psi$  synthase domain (Fig. S4A). The *tcd3* mutation site occurred in the  $\Psi$  synthase domain, which led to a change in the protein sequence and the destruction of its three-dimensional structure (Fig. S4B).

In addition, we searched various databases for sequences with similarity to each of the 11 *E. coli*  $\Psi$  synthases and found 22 homologous sequences in rice (Fig. S5). A phylogenetic tree showing the relationships of *E. coli*  $\Psi$  synthases, *Arabidopsis thaliana* SVR1 (At2g39140; involved in chloroplast rRNA processing)<sup>15</sup>, and *Chlamydomonas*  $\Psi$  synthase (Maa2)<sup>14</sup> is shown in Fig. S6. Based on the results of phylogenetic analysis, TCD3 belongs to the RsuA family and shares the greatest sequence similarity with SVR1 (Fig. S5).

Further study showed that TCD3 is conserved in higher plants, especially in millet, maize, two ear small grass, and sorghum, with similarities of 79.3%, 76.5%, 77.5%, and 79.3%, respectively (Fig. 6B). Phylogenetic analyses

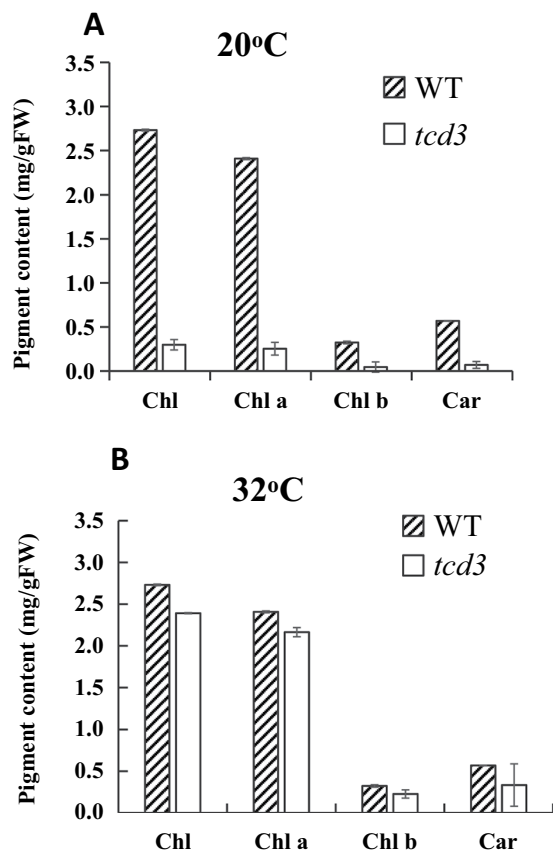


**Figure 2.** Pigment contents in the third leaves of WT and *tcd3* grown at 20° (A) and 32° (B), Chl, total chlorophyll; Chl a, chlorophyll a, Chl b, chlorophyll b; Car, carotenoid.

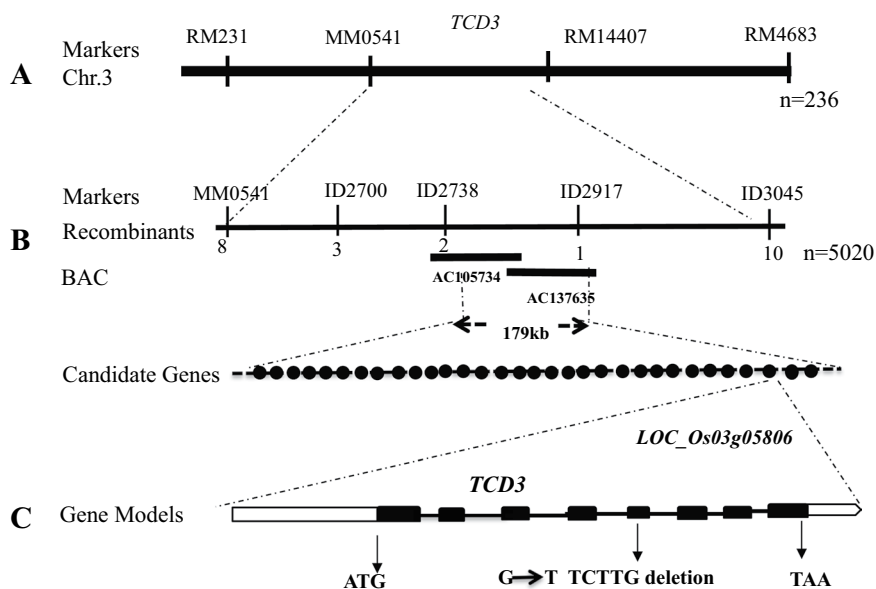


**Figure 3.** Cloning of the *TCD3* gene; (A), *TCD3* was initially localized to a region between SSR markers MM0541 and RM14407 on chromosome 3 using 236 F<sub>2</sub> mutant individuals; (B), *TCD3* was narrowed down to a 179 kb region between ID2738 and ID2917 on BAC clones AC105734 and AC137635 using 5020 F<sub>2</sub> mutant individuals; (C), gene model of *TCD3*.

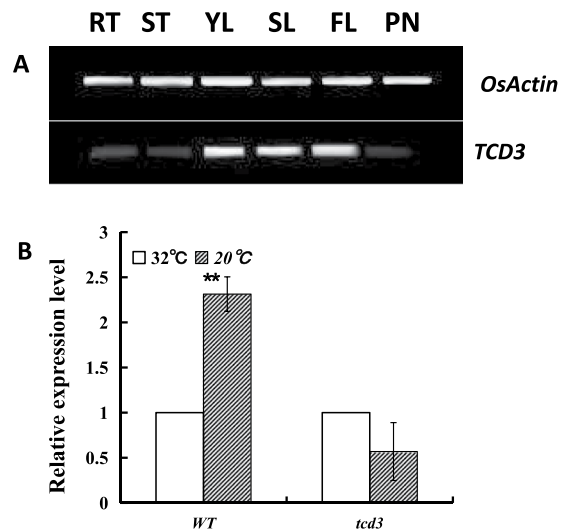


**Figure 4.** Transcript levels of *TCD3* in various tissues (**A**) and at different temperatures (**B**) determined by RT-PCR analysis; YR, young-seedling roots; ST, young-seedling stems; YL, young-seedling leaves; SL, the second leaf from the top; FL, flag leaf at heading; PN, young panicles. *OsActin* was used as a control (28 cycles for *OsActin*, 35 cycles for *TCD3*); Transcript levels (**B**) of *TCD3* in WT and *tcd3* at the 3-leaf stage at 20° and 32°, *OsActin* was used as a control for qPCR. Data are means  $\pm$  SD (n = 3). Asterisks indicate statistically significant difference compared with WT. \*\* $P < 0.01$  by Student's t-test.

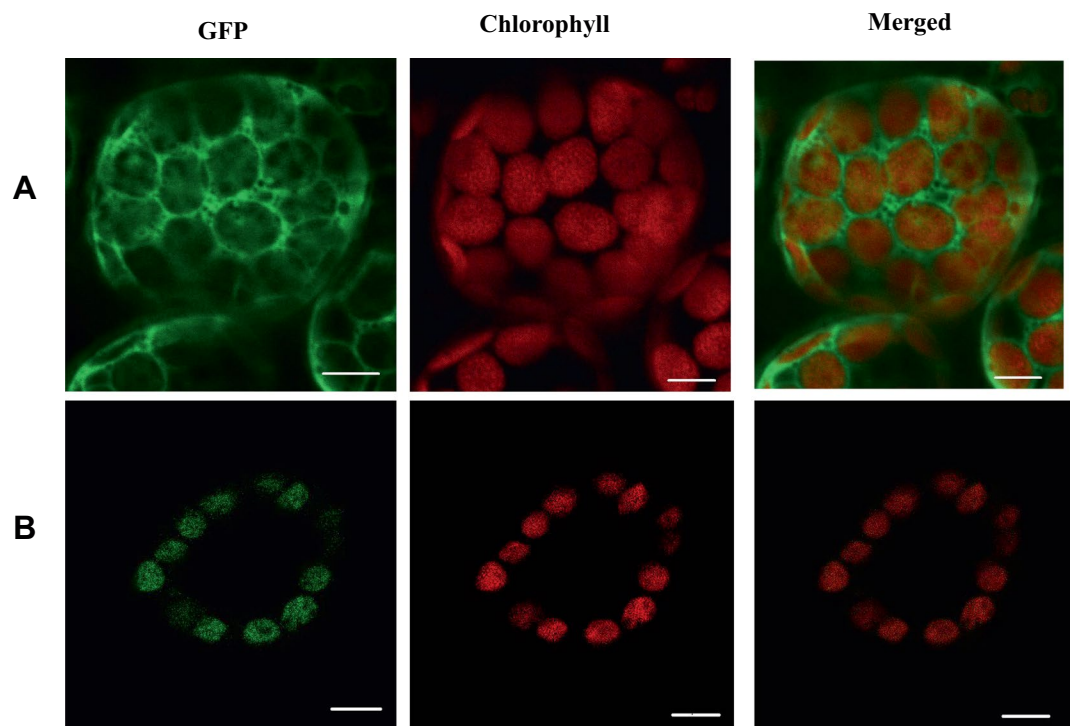


**Figure 5.** Subcellular localization of *TCD3*; (**A**) Empty GFP vector without a specific targeting sequence; (**B**) *TCD3*-GFP fusion protein; the scale bar represents 20  $\mu$ m.

showed that the *TCD3* homologs could be clearly divided into two groups: monocotyledons and dicotyledons, which conforms with the taxonomy (Fig. 6A).

**The disruption of *TCD3* alters the transcript levels of related genes.** To determine the effect of the *tcd3* mutation on the expression of genes related to chloroplast development and to explore the underlying pathway, we carried out RT-qPCR analysis of genes involved in Chl biosynthesis, photosynthesis, and chloroplast development in rice. At both high and low temperatures, low levels of *TCD3* transcripts were detected in *tcd3*, confirming



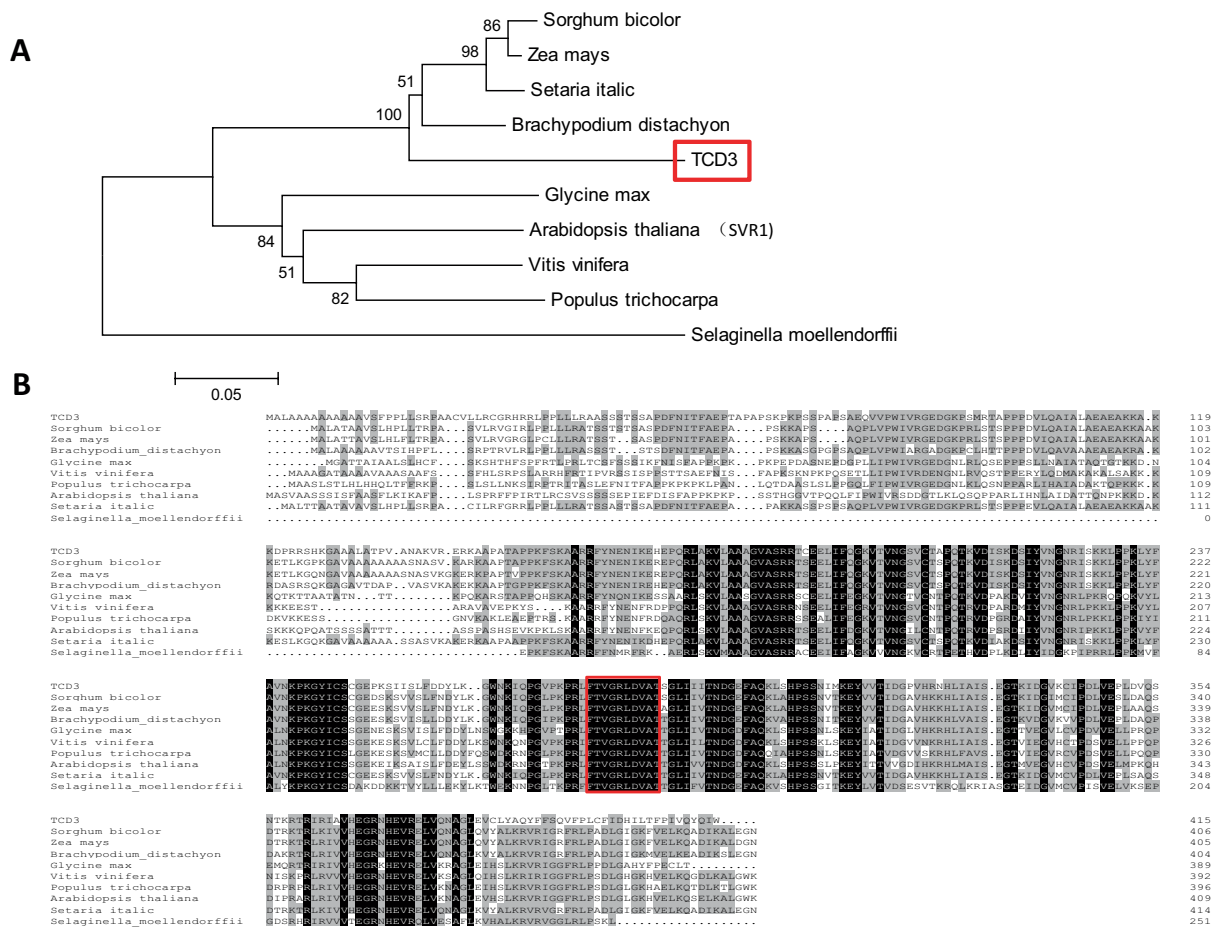


**Figure 6.** Phylogenetic analysis of TCD3 and its homologs (A); Protein sequences are from *Sorghum bicolor* (8080543), *Zea mays* (100285657), *Setaria italic* (101780537), *Brachypodium distachyon* (100846238), *Arabidopsis thaliana* (At2g39140), *Glycine max* (100808046), *Vitis vinifera* (100247893), *Populus trichocarpa* (POPTR\_0008s03540g), and *Selaginella moellendorffii* (SELMODRAFT\_45172). Scale represents percentage substitutions per site. The rooted tree is based on multiple sequence alignment using MAFFT and was generated with MEGA 6; Amino acid sequence alignment of TCD3 with its nine homologs (B). Fully and partially conserved amino acids are shaded in black and gray, respectively. The homologous comparison is based on multiple sequence alignment using MAFFT and was generated with the program DNAMAN8.

that the *tcd3* mutation blocks the transcription of this gene (Figs. 7C and 8C). At 20°C, Chl biosynthesis (*CAO*, *YGL1*, *Cab1R*) and photosynthesis (*rbcS*, *rbcL*, *psaA*, *psbA*, *LHCPII*)-related genes were significantly downregulated in *tcd3*, although *PORA* (Fig. 7A–C) was not, which is consistent with the chlorosis symptoms observed at low temperatures. Among chloroplast development-associated genes, except for *Ftsz* (encoding a component of the plastid division machinery)<sup>18,19</sup>, *V3* (*RNRL*, encoding the large subunit of ribonucleotide reductase)<sup>18</sup>, and *rps7* (encoding the small subunit ribosomal protein S7), which were upregulated in *tcd3* at 20°C, all remaining genes were strongly downregulated in the mutant. In particular, several genes were severely downregulated, including *atpA*, encoding an ATP synthase subunit<sup>20</sup>; *OsPOLP*, encoding a plastidial DNA polymerase<sup>22</sup>; *rpoC1*, encoding RNA polymerase β′ subunit; S4, encoding ribosomal protein subunit S4; and *16SrRNA* and *23SrRNA*, encoding the large (16S) and small (23S) subunits of chloroplast ribosomes, respectively. Notably, however, the transcript levels of all up- and downregulated genes in *tcd3* at 20°C were restored to WT levels at 32°C, and other genes were also expressed at WT levels when grown at 32°C (Fig. 8A–C) (within a twofold range), which corresponds with the thermo-sensitivity of the mutant phenotype. In summary, the *tcd3* mutation reduces the mRNA levels of certain genes involved in Chl biosynthesis and photosynthesis, as well as chloroplast development, at low temperatures.

## Discussion

In the current study, we identified and characterized TCD3, a pseudouridine ( $\Psi$ ) synthase required for chloroplast development at low temperatures in rice. Plants with a loss of function of *TCD3* produced imperfect chloroplasts and exhibited a Chl-deficient phenotype at low temperatures, resulting from the abnormal expression of genes associated with Chl biosynthesis, photosynthesis, and chloroplast development. Our results provide evidence that cold-induced *TCD3* plays an important role in chloroplast development in rice at low temperatures.

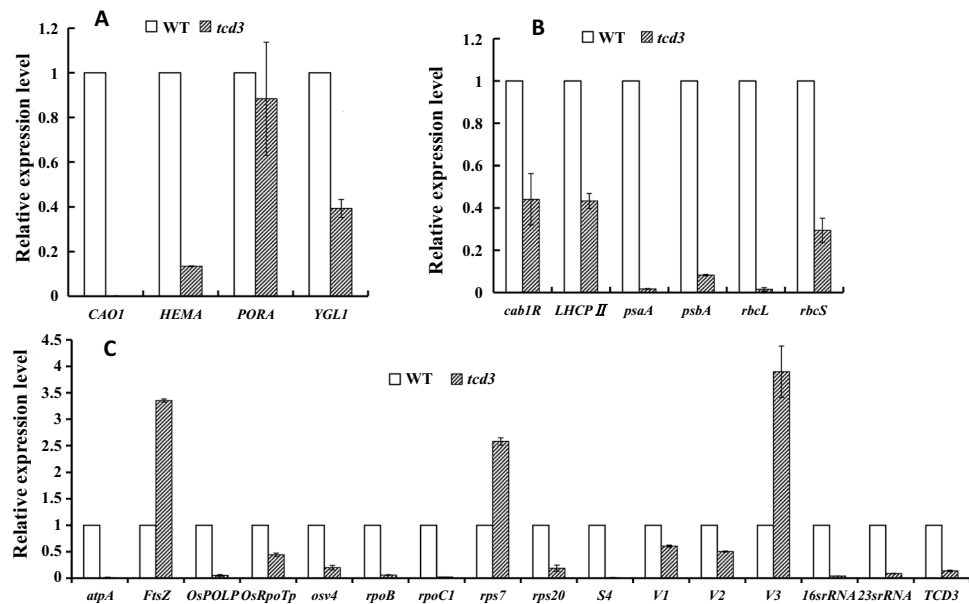


**Figure 7.** qRT-PCR analysis of genes associated with Chl biosynthesis (A), photosynthesis (B), and chloroplast development in wild type (WT) and *tcd3* at the 3-leaf stage at 20°C; the relative expression level of each gene in WT and *tcd3* was analyzed by qRT-PCR and normalized using *OsActin* as an internal control. Data are means  $\pm$  SD (n = 3).

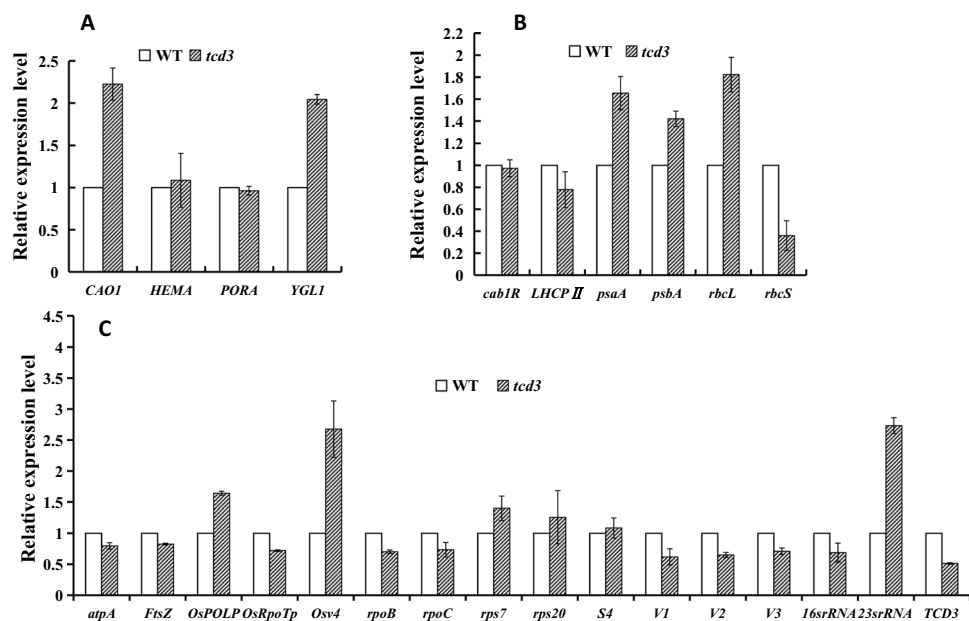


**Figure 8.** qRT-PCR analysis of genes associated with Chl biosynthesis (A), photosynthesis (B), and chloroplast development in wild type (WT) and *tcd3* at the 3-leaf stage at 32°C; the relative expression level of each gene in WT and *tcd3* was analyzed by qRT-PCR and normalized using *OsActin* as an internal control. Data are means  $\pm$  SD (n = 3).

### TCD3 regulates the first stage of chloroplast development in rice at low temperatures.

Chloroplast development in rice, which is coordinately regulated by plastid and nuclear genes, can be divided into three stages<sup>2–4</sup>. The first stage involves *OsPOLP1* (encoding a plastidial DNA polymerase) and *FtsZ* (encoding a component of the plastid division machinery)<sup>18,20</sup>. The second stage involves *OsRpoTp* (encoding a NEP), *V2* (encoding a plastidial guanylate kinase), and *rpoA* (encoding a PEP subunit)<sup>19–22</sup>. The third stage involves PEP-transcribed plastid genes (e.g., *psbA*, *rbcL*)<sup>3</sup>. Other mutants with phenotypes similar to the cold-sensitive phenotype of *tcd3* have also been reported, including the *v1*, *v2*, *v3*, *tcd9*, *osv4*, *tcd5*, *tcd10*, and *tcd11*, *tsv3* and *tcm1* mutants<sup>19,23–30</sup>. In detail, *V1* encodes the chloroplast-localized protein NUS1, which is involved in regulating

chloroplast RNA metabolism at the second stage of chloroplast development<sup>3</sup>. V2, encoding plastid or mitochondrial guanylate kinase (pt/GK), is required for the second stage of chloroplast development<sup>19</sup>. V3, encoding the large subunit of ribonucleotide reductase, is required for the first stage of chloroplast development<sup>31</sup>. More recently, we identified five additional genes that are essential for chloroplast development at low temperature: *TCD9*, encoding the  $\alpha$  subunit of chaperonin protein 60<sup>25</sup>; *OsV4* and *TCD10*, both encoding PPR proteins<sup>26,28</sup>; *TCD5*, encoding a monoxygenase<sup>32</sup>; *TCD11*, encoding plastid ribosomal protein S6<sup>27</sup>; and *TSV3*, encoding Spo0B-associated GTP-binding (Obg) protein<sup>29</sup>. Among these, *OsV4*, *TCD5*, *TCD10*, and *TCD11* participate in regulating the second stage of chloroplast development, while *TCD9* and *TSV3* participate in the first stage. In this study, the high levels of *TCD3* transcript (Fig. 4B) detected at 20 °C indicate that *TCD3* is a cold-inducible gene that is required for chloroplast development under cold stress. Notably, in *tcd3* plants at 20 °C, we detected severely reduced transcript levels (Fig. 8C) of *OsPOLP1*, which is involved in the first step of chloroplast development<sup>20,22</sup>, indicating that TCD3 regulates the first stage of chloroplast development in rice. Similarly, the transcript levels of *OsRpoTp* (encoding a NEP), as well as NEP-dependent genes (*16S rRNA*, *23S rRNA*, *rps20*, *rpoB*, *rpoC1*, *V1*, *V2*), PEP- and NEP-dependent *atpA* (which functions in the second stage of chloroplast development), and PEP-regulated plastid genes (*Cab1R*, *LHCP11*, *psaA*, *psbA*, *rbcL*, and *rbcS*, which function in the third stage of chloroplast development) were also severely reduced in the mutant under cold stress (Fig. 7). Perhaps the increased mRNA levels of *Ftsz* and *V3* during the first stage of chloroplast development and of *rps7* during the second stage are due to feedback effects. In addition, the recovery of the expression levels of all affected genes at 20 °C to WT levels in *tcd3* at 32 °C likely accounts for the normal phenotype of the mutant at 32 °C (Fig. 8A–C). The low expression level of *TCD3* at 32 °C and the high expression level at 20 °C suggest that TCD3 is indispensable for chloroplast development at low temperatures but not at high temperatures. Therefore, we conclude that TCD3 functions in the first stage of chloroplast development at low temperatures.

**Possible role of TCD3 in chloroplast rRNA and tRNA metabolism at low temperatures.** In this study, we identified the first  $\Psi$  synthase, TCD3, in rice. As mentioned above,  $\Psi$  synthases can be divided into five families. Based on the presence of an S4 domain and a  $\Psi$  synthase domain (Fig. S5A) and the results of homology analysis, TCD3 belongs to the RsuA family, members of which isomerize U (uridine) 516 in rRNA<sup>11</sup>. *TCD3* proteins also share a conserved nine-amino acid motif (GRLDVATSG; Fig. 6B) at the active site that includes a universally conserved Asp (D) residue<sup>33</sup>. In addition, the most similar protein to TCD3 is *Arabidopsis thaliana* SVR1 (60.6% sequence similarity; Fig. S6), which shares the same domains. In addition to playing a role in uridine isomerization, SVR1 is also required for proper chloroplast rRNA processing and tRNA metabolism<sup>15</sup>. Surprisingly, like 16 S rRNA and 23 S rRNA (both related to chloroplast rRNA processing), the levels of nuclear (*rbcS*, *Lhcp11*) and plastid (*rbcL*, *psaA*, *atpA*) gene expression were severely impaired in both *svr1*<sup>15</sup> and *tcd3* (Fig. 7C). In *tcd3* plants, the transcript levels of two other ribosomal protein genes (*rps20* and *S4*) were also severely reduced. Thus, TCD3, like SVR1, might play a role in chloroplast rRNA processing and tRNA metabolism at low temperatures. Therefore, under cold stress, the *tcd3* mutation affects chloroplast rRNA processing and tRNA metabolism, which in turn leads to the production of yellowish white leaves. Accordingly, the loss of TCD3-mediated *OsPOLP1*-16S-23S rRNA mRNA expression might lead to the thermo-sensitive phenotype observed under cold stress. Why does *TCD3* exhibit thermo-sensitivity? Perhaps different  $\Psi$  synthases utilize different mechanisms during environmental responses. For example, *Chlamydomonas reinhardtii* *Maa2*, which is homologous to *LOC\_Os3g26440* (Fig. S5), is highly photosensitive<sup>14</sup>, in contrast to the thermo-sensitivity of *TCD3*. The findings highlight the notion that even highly conserved genes within the same species or across species might play more diverse, complex roles than previously recognized. Under high temperature conditions, perhaps *TCD3* is not required for chloroplast development because the function of *TCD3* is replaced by that of other homologous genes (Fig. S5). Finally, our observations provide evidence for the versatile roles of plant  $\Psi$  synthases in development. Taken together, our results indicate that *TCD3* is required for chloroplast development during the early stages of leaf development in rice under cold stress.

## Materials and methods

**Plant materials and growth conditions.** The thermo-sensitive chlorophyll-deficient *tcd3* mutant was derived from *japonica* rice variety Jiahua 1 (WT) treated with <sup>60</sup>Co gamma-radiation. This thermo-sensitive leaf color mutant exhibits leaf yellowing at low temperatures. The F<sub>2</sub> mapping population was generated from a cross between Pe'ai 64S (*indica*) and *tcd3*. All rice seedlings were grown in growth chambers under controlled conditions with a 12-h-dark/12-h-light cycle at 20 °C or 32 °C.

**Phenotypic characterization and measurement of photosynthetic pigments.** Germinated seeds of *tcd3* and Jiahua 1 (WT) were sown on soils under controlled conditions as described above at 20 °C or 32 °C. The 3<sup>rd</sup> leaves (200 mg) from plants at the three-leaf stage were homogenized in 10 mL of 100% acetone. The absorbance value of the supernatant at 470, 645, and 663 nm was determined by spectrophotometry (Beckman Coulter, Danvers, MA, USA). The chlorophyll (Chl) and carotenoid (Car) contents were determined by spectrophotometry as described by Arnon<sup>34</sup> and Wellburn<sup>35</sup>. In addition, WT and *tcd3* plants were grown in a paddy field at Shanghai Normal University, China, in 2010. Leaf Chl SPAD values (Fig. S1) were measured using a chlorophyll meter (SPAD-502, Minolta Co. Ltd., Japan), a nondestructive, rapid method for estimating photosynthetic pigment levels<sup>36–38</sup>. The SPAD values were measured every week from transplantation (summer) to the heading (autumn) stage. Various yield-associated traits (Fig. S2) were investigated at maturity.

**Observation of chloroplast structure by transmission electron microscopy (TEM).** Chloroplast development was observed in the third leaves of WT and *tcd3* plants using TEM as described elsewhere<sup>39</sup> with minor modifications. Briefly, the third leaves were sampled from seedlings at the 3-leaf-stage grown at 20 °C



and 32 °C. Transverse leaf sections were fixed in 2.5% glutaraldehyde solution at 4° for 4 h, rinsed and incubated overnight in 1% w/v OsO<sub>4</sub> at 4°, and embedded in Epon 812 resin. The samples were stained again and examined under a Hitachi-7650 transmission electron microscope.

**Positional cloning of *TCD3*.** Genomic DNA was extracted from rice leaves using an improved CTAB method<sup>40</sup>. Initially, 236 F<sub>2</sub> recessive seedlings from the cross Pei'ai 64 S/*tcd3* were used to identify the molecular markers linked to the mutant gene. Subsequently, 5020 F<sub>2</sub> plants showing the mutant phenotype were used for fine mapping. New molecular markers were designed by comparing the sequences of 93–11<sup>41</sup> and Nipponbare<sup>42</sup> from NCBI (<http://www.ncbi.nlm.nih.gov>); the markers are listed in Table S2.

**Complementation of the *tcd3* mutant.** For the complementation test, genomic DNA was extracted from WT plants and used as a PCR template with the primer pair TCD3F: 5'-GGGGTACCGCCCATACAGATCCTCG-3' (*KpnI*) and TCD3R: 5'-GCGTCGACTTTCAGCAAACCCCATG-3' (*Sall*), amplifying a fragment (6.9 kb) containing the target gene (*TCD3*) and the 1.5 kb upstream and 0.35 kb downstream sequences. The PCR products were cloned into the pMD18-T vector (TaKaRa, Dalian, China). The pMD18T-*TCD3* construct was digested with *KpnI* and *Sall* and ligated into the *KpnI* and *Sall* site of binary vector pCAMBIA1301 (CAMBIA, <http://www.cambia.org.au>). The resulting pCAMBIA1301:*TCD3* vector was transferred into *Agrobacterium tumefaciens* strain EHA105 and introduced into the *tcd3* mutant by *Agrobacterium*-mediated transformation according to previously published methods<sup>43</sup>, except that the temperature used for *in vitro* plant differentiation was 20 °C. The genotypes of the transgenic seedlings were determined by PCR amplification of the hygromycin phosphotransferase gene (*hpt*) with primers HPTF (5'-GGAGCATATACGCCCGGAGT-3') and HPTR (5'-GTTTATCGGCACTTTCATCG-3') and primers GUSF (5'-GGGATCCATCGCAGCGTAATG-3') and GUSR (5'-GCCGACAGCAGCAGTTTCATC-3') as selection markers. The resulting T<sub>0</sub> transgenic seedlings were grown in a paddy field after screening for hygromycin-tolerant plants and confirmation by DNA sequencing. All T<sub>1</sub> seedlings were grown at 20° and used to examine the segregation of the mutant phenotype.

**Knockout of *TCD3*.** To experimentally affirm that *TCD3* is responsible for the phenotypic changes observed in *tcd3*, CRISPR/Cas9 genome editing was performed on WT plants. To generate the Cas9 targeting construct for *TCD3* using CRISPR Primer Designer software (<http://www.crispr.dbcls.jp/>)<sup>44</sup>, annealed gRNA oligonucleotide pairs with recognition sequences were designed (F1: 5'-GCCGGACTTCAACATCACCTTCG-3', R1: 5'-AAACCGAAGGTGATGTTGAAGTC-3'; F2: GCCGGACTTCAACATCACCTTCG, R2: AAACCGAAGGTGATGTTGAAGTC; F3: GCCGCTGCGTGCTCCTCCGCTG, R3: AAACGACGGAGGACACGCAGG; F4: GCCGGCGGAGGCGGAGGCCAAGA). The recognition sequences were inserted into the region between the OsU6 promoter and the gRNA scaffolds (from the pYLgRNA-OsU6 vector) of the Cas9 expression backbone vector (pYL-CRISPR/Cas9-MH) at the *BsaI* sites as previously described<sup>45</sup>. The resulting plasmid (CRISPR/Cas9 expression) and the empty vector were introduced into *Agrobacterium* strain EHA105 and used to infect calli from WT plants<sup>43</sup>. The resulting T<sub>1</sub> seedlings were grown and used to examine the segregation of the mutant phenotype at 20 °C.

**Subcellular localization.** To investigate the subcellular localization of TCD3, cDNA fragments encoding the 144 amino-acid N-terminal region of *TCD3* were amplified from total RNA extracts using following primers (5'-GAAGATCTATGGCCCTCGCCGCCGCCGCCGCCGCG-3' and 5'-GGGGTACCCCTCTCCCTCACCTTGGCAT-3') and introduced into vector pMON530-GFP at the *BglII* and *KpnI* sites (the underlined sequences represent cleavage sites). The resulting pMON530:CaM-V35S:TCD3-GFP plasmid was verified by sequencing and introduced into *Agrobacterium* strain EHA105. The localization of TCD3 was investigated by transient expression analysis of the GFP fusion protein in tobacco (*Nicotiana tabacum*) cells via confocal microscopy as described previously<sup>25</sup>. GFP fluorescence in the transformed protoplasts was imaged by confocal laser-scanning microscopy (LSM5 PASCAL; ZEISS, <http://www.zeiss.com>).

**RT-PCR and quantitative RT-PCR (qRT-PCR) analysis.** Total RNA from WT plants was extracted from seedling roots (ST), young stems (YS), the third leaves of plants at the 3-leaf stage, the second leaves (SL) from the tops of plants, and flag leaves (FL) and young panicles (PN) from plants at the heading stage using an RNA Prep Pure Plant kit (Tiangen Co., Beijing, China) to investigate the tissue-specific expression patterns of *TCD3*. The RNA was reversely transcribed into cDNA and used for RT-PCR as described previously<sup>25</sup>. In addition, RNA from the third leaves of WT and *tcd3* seedlings at the 3-leaf stage grown at 20 °C and 32 °C was extracted as described above and used to measure the transcript levels of *TCD3* as well as Chl biosynthesis, chloroplast development, and photosynthesis-associated genes (*atpA*, *Cab1R*, *CAO*, *FtsZ*, *HEMA*, *LHCPII*, *OsPOLP*, *OsRpoTp*, *OsV4*, *PORA*, *psaA*, *psbA*, *rbcl*, *rbclS*, *rpoB*, *rpoC*, *rps7*, *rps20*, *RNRL*, *S4*, *V1*, *V2*, *YGL-1*, *16SrRNA*, *23SrRNA*) in rice. The qPCR was performed using a SYBR Premix Ex Taq™ kit (TaKaRa) on an ABI7500 Real-Time PCR System (Applied Biosystems; <http://www.appliedbiosystems.com>), and the relative quantification of gene expression data was performed as described in Livak and Schmittgen<sup>46</sup>. The specific primers for qPCR were partially referred to Wu *et al.*<sup>47</sup> based on sequences from NCBI; the primers are listed in Table S3. The rice *OsActin* gene was used as a reference gene.

**Sequence and phylogenetic analyses.** Gene prediction and structure analysis were carried out using the GRAMENE database (<http://www.gramene.org>). Homologs of TCD3 were identified by BLASTP analysis against the National Center for Biotechnology Information database (<http://www.ncbi.nlm.nih.gov>) and subjected to multiple sequence alignment using DNAMAN version 6.0 (Lynnsoft Biosoft, USA). The signal peptide was predicted with SignalP version 2.0<sup>47</sup>. The phylogenetic tree was constructed using MEGA version 6 software (<http://www.megasoftware.net>).

Received: 2 September 2019; Accepted: 8 April 2020;

Published online: 22 May 2020

## References

- Von, C. S., Quick, W. P. & Furbank, R. T. The development of C4 rice: current progress and future challenges. *Science* **336**, 1671–1672 (2012).
- Kusumi, K., Chono, Y., Gotoh, E., Tsuyama, M. & Iba, K. Chloroplast biogenesis during the early stage of leaf development in rice. *Plant Biotechnol. J.* **27**, 85–90 (2010).
- Kusumi, K., Sakata, C., Nakamura, T. & Kawasaki, S. A plastid protein NUS1 is essential for build-up of the genetic system for early chloroplast development under cold stress conditions. *Plant J.* **68**, 1039–1050 (2011).
- Kusumi, K. & Iba, K. Establishment of the chloroplast genetic system in rice during early leaf development and at low temperatures. *Front Plant Sci.* **5**, 1–6 (2014).
- Beale, S. I. Green genes gleaned. *Trends in Plant Science* **10**, 309–312 (2005).
- Morita, R., Sato, Y., Masuda, Y., Nishimura, M. & Kusaba, M. Defect in non-yellow coloring 3, an alpha/beta hydrolase fold family protein, causes a stay-green phenotype during leaf senescence in rice. *Plant J.* **59**, 940–952 (2009).
- Terry, M. J. & Kendrick, R. E. Feedback inhibition of chlorophyll synthesis in the phytochrome chromophore-deficient aurea and yellow-green-2 mutants of tomato. *Plant Physiol.* **119**, 143–152 (1999).
- Chen, G., Bi, Y. R. & Li, N. EGY1 encodes a membrane-associated and ATP-independent metalloprotease that is required for chloroplast development. *Plant J.* **41**, 364–375 (2005).
- Kushnir, S. *et al.* A mutation of the mitochondrial ABC transporter Sta1 leads to dwarfism and chlorosis in the *Arabidopsis* mutant starik. *Plant Cell* **13**, 89–100 (2001).
- Pfalz, J. & Pfannschmidt, T. Essential nucleoid proteins in early chloroplast development. *Trends Plant Sci.* **18**, 186–194 (2013).
- Hamma, T. & Ferré-D'Amaré, A. R. Pseudouridine synthases. *Chem. Biol.* **13**, 1125–1135 (2006).
- Kaya, Y. & Ofengand, J. A novel unanticipated type of pseudouridine synthase with homologs in bacteria archaea and eukarya. *RNA* **9**, 711–721 (2003).
- Gutgsell, N. *et al.* Deletion of the *Escherichia coli* pseudouridine synthase gene *truB* blocks formation of pseudouridine 55 in tRNA *in vivo*, does not affect exponential growth, but confers a strong selective disadvantage in competition with wild-type cells. *RNA* **6**, 1870–1881 (2000).
- Perron, K., Goldschmidt-Clermont, M. & Rochaix, J. A factor related to pseudouridine synthases is required for chloroplast group II intron trans-splicing in *Chlamydomonas reinhardtii*. *Embo. J.* **18**, 6481–6490 (1999).
- Yu, F., Liu, X., Alsheikh, M., Park, S. & Rodermeier, S. 2008 Mutations in suppressor of variegation1, a factor required for normal chloroplast translation, suppress var2-mediated leaf variegation in *Arabidopsis*. *Plant Cell* **20**, 1786–804 (2008).
- Emanuelsson, O., Nielsen, H. & Brunak, S. 2000 Predicting subcellular localization of proteins based on their N-terminal amino acid sequence. *J. Mol. Biol.* **300**, 1005–1016 (2000).
- Finn, R. D. *et al.* The Pfam protein families database. *Nucleic Acids Res.* **38**, 211–222 (2010).
- Yoo, Y. *et al.* Rice *Virescent3* and *Stripe1* encoding the large and small subunits of ribonucleotide reductase are required for chloroplast biogenesis during early leaf development. *Plant Physiol.* **150**, 388–401 (2009).
- Vitha, S., McAndrew, R. S. & Osteryoung, K. W. FtsZ ring formation at the chloroplast division site in plants. *J. Cell Biol.* **153**, 111–120 (2001).
- Hiratsuka, J., Shimada, H., Whittier, R., Ishibashi, T. & Sakamoto, M. The complete sequence of the rice (*Oryza sativa* L.) chloroplast genome: intermolecular recombination between distinct tRNA genes accounts for a major plastid DNA inversion during the evolution of the cereals. *Mol. Gen. Genet.* **217**, 185–194 (1989).
- Kusumi, K., Yara, A., Mitsui, N., Tozawa, Y. & Iba, K. Characterization of a rice nuclear-encoded plastid RNA polymerase gene *OsRpoTp*. *Plant Cell Physiol.* **45**, 1194–1201 (2004).
- Iba, K., Takamiya, K., Toh, Y., Satoh, H. & Nishimura, M. Formation of functionally active chloroplast is determined at a limited stage of leaf development in virescent mutants of rice. *Devel. Genet.* **12**, 342–348 (1991).
- Kusumi, K., Mizutani, A., Nishimura, M. & Iba, K. A *Virescent* gene *v1* determines the expression timing of plastid genes for transcription translation apparatus during early leaf development in rice. *Plant J.* **12**, 1241–1250 (1997).
- Jiang, Q. *et al.* Importance of the rice *TCD9* encoding a subunit of chaperonin protein60 (Cpn60 $\alpha$ ) for the chloroplast development during the early leaf stage. *Plant Sci.* **215–216**, 172–179 (2014).
- Gong, X. *et al.* The rice *OsV4* encoding a novel pentatricopeptide repeat protein is required for chloroplast development during the early leaf stage under cold stress. *J. Integr. Plant Biol.* **56**, 400–410 (2014).
- Wang, W. *et al.* The rice *TCD11* encoding plastid ribosomal protein S6 is essential for chloroplast development at low temperature. *Plant Science* **259**, 1–11 (2017).
- Wu, L. *et al.* The rice pentatricopeptide repeat gene *TCD10* is needed for chloroplast development under cold stress. *Rice* **9**, 67 (2016).
- Lin, D. *et al.* Rice *TSV3* encoding Obg-like GTPase protein is essential for chloroplast development during the early leaf stage under Cold Stress. *G3 (Bethesda)* **8**, 253–263 (2018).
- Lin, D. *et al.* *TCM1* encoding a component of TAC complex is required for chloroplast development under cold stress. *The Plant Genome* **11**(1), 1–13 (2018).
- Yoo, S. C. *et al.* Rice *Virescent3* and *Stripe1* encoding the large and small subunits of ribonucleotide reductase are required for chloroplast biogenesis during early leaf development. *Plant Physiol.* **150**, 388–401 (2009).
- Wang, F. *et al.* Temperature-sensitive albino gene *TCD5*, encoding a monooxygenase, affects chloroplast development at low temperatures. *Journal of Experimental Botany* **67**(17), 5187–5202 (2016).
- Ofengand, J. Ribosomal RNA pseudouridines and pseudouridine synthases. *Febs Lett.* **514**, 17–25 (2002).
- Arnon, D. I. Copper enzymes in isolated chloroplasts. *Plant Physiol.* **24**, 1–15 (1949).
- Wellburn, A. R. The spectral determination of chlorophylls a and b, as well as total carotenoids, using various solvents with spectrophotometers of different resolution. *J. Plant Physiol.* **144**, 307–313 (1994).
- Peng, S., Garcia, F. V., Lasa, R. C. & Classman, K. G. Adjustment for specific leaf weight improves chlorophyll meter's estimate of rice leaf nitrogen concentration. *Agron J.* **85**, 987–990 (1993).
- Turner, F. T. & Jund, M. F. Chlorophyll meter to predict nitrogen topdress requirement for semidwarf rice. *Agron J.* **83**, 926–928 (1991).
- Dwyer, L. M., Tollenaar, M. & Houwing, L. A nondestructive method to monitor leaf greenness in corn. *Can J. Plant Sci.* **71**, 505–509 (1991).
- Inada, N., Sakai, A., Kuroiwa, H. & Kuroiwa, T. Three-dimensional analysis of the senescence program in rice (*Oryza sativa* L.) coleoptiles. *Planta* **206**, 585–597 (1998).
- Murray, M. G. & Thompson, W. F. Rapid isolation of high molecular weight plant DNA. *Nucleic Acids Res.* **8**, 4321–4326 (1980).
- Yu, J. *et al.* A draft sequence of the rice genome (*Oryza sativa* L. Ssp. indica). *Science* **296**, 79–92 (2002).
- Goff, S. A. *et al.* A draft sequence of the rice genome (*Oryza sativa* L. ssp. japonica). *Science* **296**, 92–100 (2002).

42. Hiei, Y., Ohta, S., Komari, T. & Kumashiro, T. Efficient transformation of rice (*Oryza sativa* L.) mediated by Agrobacterium and sequence analysis of the boundaries of the T-DNA. *Plant J.* **6**, 271–282 (1994).
43. Naito, Y., Hino, K., Bono, H. & Ui-Tei, K. CRISPRdirect: software for designing CRISPR/Cas guide RNA with reduced off-target sites. *Bioinformatics* **31**, 1120–1123 (2015).
44. Ma, X. *et al.* A robust CRISPR/Cas9 system for convenient, high-efficiency multiplex genome editing in monocot and dicot plants. *Mol. Plant* **8**, 1274–1284 (2015).
45. Livak, K. J. & Schmittgen, T. D. Analysis of relative gene expression data using real-time quantitative PCR and the 2<sup>(-Delta Delta C(T))</sup> Method. *Methods* **25**, 402–408 (2001).
46. Wu, Z. M. *et al.* A chlorophylldeficient rice mutant with impaired chlorophyllide esterification in chlorophyll biosynthesis. *Plant Physiol.* **145**, 29–40 (2007).
47. Nielsen, H. & Krogh, A. Prediction of signal peptides and signal anchors by a hidden Markov model. *Proc. Int. Conf. Intell. Syst. Mol. Biol.* **6**, 122–130 (1998).

## Acknowledgements

We sincerely thank Dr. Nancy Hofmann for her critical reading of and suggestions for our manuscript. We are grateful to Prof. Zhongnan Yang for kindly providing pMON530-GFP vector and for his constructive comments as well. The project was financially supported by Minister of Science and Technology of China (MOST) (2016YFD0100902), the Shanghai Municipal Science and Technology Commission (19391900200 and 16391900700), Innovation Program of Shanghai Municipal Education Commission (2017-01-07-00-02-E00039), the Natural Science Foundation of China (No. 30971552), and International Cooperation Project of South Korea and China (PJ013647).

## Author contributions

D.L. and Y.D. provided the mutant rice seeds. R.K., D.L., L.W., J.X. and Y.D. generated F<sub>2</sub> and F<sub>3</sub> seeds for genotyping and phenotyping. R.K., L.W., L.C., Y.W., D.L. and Y.D. performed the experiments of phenotype assays and molecular analysis. R.K., D.L., Y.D., Z.P. and G.L. designed and discussed the research plan. R.K., D.L. and Y.D. wrote the manuscript. All authors approved the manuscript.

## Competing interests

The authors declare no competing interests.

## Additional information

**Supplementary information** is available for this paper at <https://doi.org/10.1038/s41598-020-65467-2>.

**Correspondence** and requests for materials should be addressed to Y.D.

**Reprints and permissions information** is available at [www.nature.com/reprints](http://www.nature.com/reprints).

**Publisher's note** Springer Nature remains neutral with regard to jurisdictional claims in published maps and institutional affiliations.



**Open Access** This article is licensed under a Creative Commons Attribution 4.0 International License, which permits use, sharing, adaptation, distribution and reproduction in any medium or format, as long as you give appropriate credit to the original author(s) and the source, provide a link to the Creative Commons license, and indicate if changes were made. The images or other third party material in this article are included in the article's Creative Commons license, unless indicated otherwise in a credit line to the material. If material is not included in the article's Creative Commons license and your intended use is not permitted by statutory regulation or exceeds the permitted use, you will need to obtain permission directly from the copyright holder. To view a copy of this license, visit <http://creativecommons.org/licenses/by/4.0/>.

© The Author(s) 2020